Available online at www.sciencedirect.com
ScienceDirect
Journal of Power Sources 162 (2006) 1165–1171
JOURNAL OF POWER SOURCES
www.elsevier.com/locate/jpowsour

Estimation of contact resistance in proton exchange membrane fuel cells

Lianhong Zhang [a], Ying Liu [a], Haimin Song [a], Shuxin Wang [a,*], Yuanyuan Zhou [b], S. Jack Hu [b]

[a] *School of Mechanical Engineering, Tianjin University, 92 Weijin Road, Nankai District, Tianjin 300072, PR China*
[b] *Department of Mechanical Engineering, The University of Michigan, Ann Arbor, MI 48109-2125, USA*

Received 29 April 2006; received in revised form 27 July 2006; accepted 27 July 2006
Available online 12 September 2006

Abstract

The contact resistance between the bipolar plate (BPP) and the gas diffusion layer (GDL) is an important factor contributing to the power loss in proton exchange membrane (PEM) fuel cells. At present there is still not a well-developed method to estimate such contact resistance. This paper proposes two effective methods for estimating the contact resistance between the BPP and the GDL based on an experimental contact resistance–pressure constitutive relation. The constitutive relation was obtained by experimentally measuring the contact resistance between the GDL and a flat plate of the same material and processing conditions as the BPP under stated contact pressure. In the first method, which was a simplified prediction, the contact area and contact pressure between the BPP and the GDL were analyzed with a simple geometrical relation and the contact resistance was obtained by the contact resistance–pressure constitutive relation. In the second method, the contact area and contact pressure between the BPP and GDL were analyzed using FEM and the contact resistance was computed for each contact element according to the constitutive relation. The total contact resistance was then calculated by considering all contact elements in parallel. The influence of load distribution on contact resistance was also investigated. Good agreement was demonstrated between experimental results and predictions by both methods. The simplified prediction method provides an efficient approach to estimating the contact resistance in PEM fuel cells. The proposed methods for estimating the contact resistance can be useful in modeling and optimizing the assembly process to improve the performance of PEM fuel cells.

Keywords: PEM fuel cells; Contact resistance; Contact pressure; Constitutive relation; FEM analysis

1. Introduction

PEM fuel cells are recognized as potentially environmentally friendly power sources for residential, portable and transportation applications [1]. Recent research has revealed that around 59% of the total power losses are due to the contact resistance between the bipolar plates (BPP) and the gas diffusion layer (GDL) in PEM fuel cells [2]. One key factor influencing the contact resistance of PEM fuel cells is the assembly pressure. Not enough assembly pressure may lead to leakage of the fuels and a high contact resistance. Too much pressure, on the other hand, increases the flow resistance and may also result in damage to the gas diffusion layer and the proton exchange membrane. Optimization of the assembly pressure is essential to the performance of PEM fuel cells. Effective prediction of the contact resistance between the BPP and the GDL is fundamental to modeling the assembly process and optimizing the assembly pressure of PEM fuel cells.

Several theoretical models for predicting the interfacial contact resistance have been developed [3–7], including the Greenwood–Williamson model [3,4], the Cooper–Mikic–Yovanovitch model [5] and the Majumdar–Tien fractal model [6,7]. One critical limitation of these models is the dependence of the geometric parameters on the resolution of the roughness-measuring instrument. And widely different values of contact resistance may be obtained for the same contact surface pair depending on the resolution setting of the profilometer device [12]. Therefore, effective theoretical models for prediction of the contact resistance in PEM fuel cells are still under development.

Experimental research on the contact resistance has been reported in the literature [8–14]. Lee et al. [8] reported the changes in fuel cell performance as a function of the compression pressure resulting from torque on the bolts that clamped the fuel cell. Three types of gas diffusion layers were studied

* Corresponding author. Tel.: +86 22 27403434; fax: +86 22 87402173.
E-mail address: shuxinw@tju.edu.cn (S. Wang).

0378-7753/$ – see front matter © 2006 Elsevier B.V. All rights reserved.
doi:10.1016/j.jpowsour.2006.07.070

at 202 kPa and 353 K, in which the performance changes may be attributed to change in electrical resistance. Ihonen et al. [9] measured the in situ contact resistance of un-plated and plated stainless steel as a function of operation time, clamping pressure, gas pressure and electric current density. Wang et al. [10] studied the contact resistance between carbon paper and stainless steel because stainless steel is considered to be a good candidate for bipolar plates due to its low cost, high strength, ease of machining and forming, as well as its corrosion resistance. Cho et al. [11] compared the performance of fuel cells with two kinds of carbon composite bipolar plates due to their different electrical and physical properties. Mishra et al. [12] investigated the effects of different GDL materials and contact pressures on the contact resistance and compared these with the results predicted by the fractal model. Lee et al. [13] conducted FEM analysis of the pressure distribution in a single cell. Jung et al. [14] reported the contact resistance of different flow field combinations in a direct methanol fuel cell. Though estimation of the contact resistance by experiments is feasible, it is expensive and time consuming.

In this paper, the contact resistance in fuel cells is estimated using two semi-empirical methods. In these methods, an experimental constitutive relation between the contact resistance and the contact pressure is obtained and then combined with simple estimation or FEM analysis of contact pressure in estimating the contact resistance. The remainder of the paper is organized as follows: Section 2 describes the methodology. Section 3 presents and compares the results from the FEM analysis, simplified prediction and experiments. Finally, Section 4 draws the conclusions.

2. Methodology

The general idea of this study is to experimentally obtain a contact resistance–pressure constitutive relation for the contact between the BPP and the GDL, and to estimate the contact pressure in a real fuel cell stack based on either geometrical relations or FEM analysis. Then, the contact resistance is estimated according to the constitutive relation and the contact pressure. The schematic of the methodology is shown in Fig. 1, which consists of three steps:

Step 1. *Experimental constitutive relation*: The experimental constitutive relation of the contact resistance–pressure relationship between the BPP and the GDL is obtained by measuring the resistance of a GDL sandwiched between two flat plates of the same material and processing conditions as the BPP under a stated contact pressure.

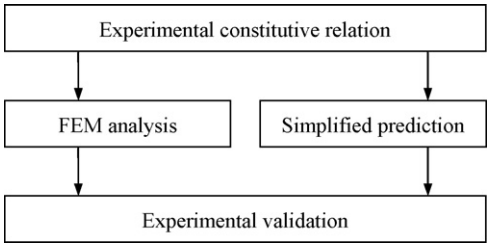

Fig. 1. Schematic plot of the methodology.

Step 2. (a) *Simplified prediction*: The contact pressure is estimated by using a simple relation of the nominal contact area and the clamping force. The resistance is obtained according to contact pressure and the experimental contact resistance–pressure constitutive relation.

(b) *FEM analysis*: FEM analysis is conducted to simulate the clamping of PEM fuel cells to obtain the contact area and contact pressure between the BPP and the GDL. The contact resistance between contact elements is calculated via the constitutive relation of contact resistance–pressure. The total contact resistance is estimated by considering all contact elements in parallel.

Step 3. *Experimental validation*: Experiments were carried out to measure the contact resistance between the practical BPP and the GDL to verify the results of two estimation methods.

2.1. Constitutive relation experiments

Electrical interface resistance of contacting conductors is dominated by multiple factors such as the physical–mechanical properties, topological status and parameters of contact surfaces, environment conditions and mechanical contact pressure. There inherently exists a complex constitutive relation between the contact resistance and its dominant factor. Unfortunately, present theoretical models for interfacial contact resistance cannot precisely represent the complex relation. This may be the essential reason why significant errors exist in theoretical models of contact resistance. Furthermore, the parameters in the theoretical models must be experimentally calibrated to a specific electrical interfacial contact.

The constitutive relation proposed in this paper directly establishes the empirical relation between interfacial contact resistance and contact pressure by experiments, which circumvent the various difficulties in dealing with the influencing factors on contact resistance.

2.1.1. Experimental setup

An experimental setup similar to Ref. [12], as shown in Fig. 2, was used to obtain the constitutive relation between the contact resistance and pressure, and to verify the prediction of contact resistance between the BPP and the GDL of PEM fuel cells. The setup consisted of a custom-made hydraulic press with a load capacity of 25 kN, a load sensor with a measurement range of 0–25 kN and an accuracy of 0.1%, a ZY9858 micro-ohmmeter with a resolution of 0.1 μΩ and accuracy of 0.1% RX and a computer system to acquire the load and resistance data. The GDL was sandwiched between two flat graphite plates of the same material and processing conditions as the BPP. The sandwiched graphite plates/GDL assembly was then placed between two gold plates, as illustrated in Fig. 2. Another similar setup with only one flat graphite plate between two gold plates was also built. Kelvin clip leads were used to connect the gold plate to

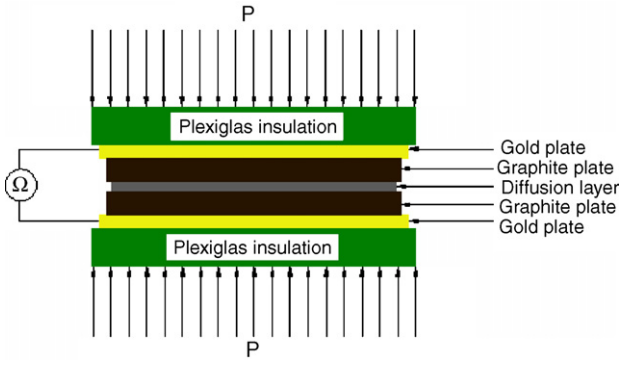

Fig. 2. Schematic plot of contact resistance measurement setup (adapted from Ref. [12]).

the micro-ohmmeter. Plexiglas layers were placed between the platens of the press and the gold plates for insulation. The micro-ohmmeter was used to measure the resistance of two setups.

2.1.2. Experimental materials and conditions

The GDL for the experiment was TGP-H-120 from Toray Industries, Inc. The flat plates were TB-8 graphite plates provided by Beijing LN-Power Sources Corp., Ltd. The physical–mechanical property parameters of the GDL and the graphite plates are listed in Tables 1 and 2. Since the bulk resistance of the GDL and the graphite plates are quite small, the change in bulk resistance due to compression is ignored.

Table 1
Physical–mechanical properties of TGP-H-120 GDL

Properties (units)	Value
Thickness (mm)	0.377
Area (cm^2)	7.9 × 7.9
Bulk density ($g\,cm^{-3}$)	0.45
Porosity (%)	78
Surface roughness R_a (μm)	8
Electrical resistivity (mΩ cm)	
Through plane	80
In plane	4.7
Flexural strength (MPa)	40
Tensile strength ($N\,cm^{-1}$)	90
Young's modulus (MPa)	6.3
Poisson's ratio	0.09

Table 2
Physical–mechanical properties of TB-8 graphite plate

Properties (units)	Value
Thickness (mm)	2.2
Area (cm^2)	8.2 × 8.2
Bulk density ($g\,cm^{-3}$)	≥1.94
Porosity (%)	≯0.12
Granule (μm)	<44
Electrical resistivity (mΩ cm)	
In plane	0.5
Through plane	4.5
Flexural strength (MPa)	51
Compression strength (MPa)	110
Young's modulus (GPa)	0.13
Poisson's ratio	0.21

In order to investigate the effect of contact pressure on contact resistance, the clamping pressure was varied from 0.5 to 3.0 MPa in the present study as compared to the typical clamping pressure of 1 MPa in PEM fuel cells. Since the graphite plate is flat, the clamping pressure applied to the assembly is equal to the contact pressure at the interface of graphite plates and GDL, and the apparent contact area is the area of gas diffusion layer. The scale of the micro-ohmmeter was set to 20 mΩ with a measuring resolution of 1 μΩ.

The experiments were carried out at room temperature, 20 °C, and 40% relative humidity.

2.1.3. Interfacial contact resistance calculation

Referring to Fig. 2, the total resistance R_{tot1} of the gold plates/flat plates/GDL assembly consists of:

(a) the bulk resistance of two flat graphite plates, $2R_{Gr}$;
(b) the bulk resistance of gas diffusion layer, R_{GDL};
(c) two interfacial contact resistances between flat graphite plate and gas diffusion layer, $2R_{Gr/GDL}$;
(d) two interfacial contact resistances between gold plate and flat graphite plate, $2R_{Au/Gr}$.

$$R_{tot1} = 2R_{Gr} + R_{GDL} + 2R_{Gr/GDL} + 2R_{Au/Gr} \quad (1)$$

The interfacial contact resistance between flat graphite plate and gas diffusion layer can be calculated as follows

$$R_{Gr/GDL} = \frac{R_{tot1} - 2R_{Gr} - R_{GDL} - 2R_{Au/Gr}}{2} \quad (2)$$

The bulk resistance of the flat graphite plates and gas diffusion layer are calculated according to their electrical resistivity. The sum of resistance R_{Gr} and $2R_{Au/Gr}$ can be measured by another setup with an assembly of gold plate/flat graphite plate/gold plate.

$$R_1 = R_{Gr} + 2R_{Au/Gr} \quad (3)$$

Thus

$$R_{Au/Gr} = \frac{R_1 - R_{Gr}}{2} \quad (4)$$

From Eqs. (2) and (4), $R_{Gr/GDL}$ can be calculated as

$$R_{Gr/GDL} = \frac{R_{tot1} - R_{Gr} - R_{GDL} - R_1}{2} \quad (5)$$

The constitutive relation of contact resistance–pressure can be obtained using the relations of R_1 and R_{tot1} with pressure attained in the two experimental setups and the constitutive contact resistance $R_{contact}$, as a function of contact pressure, is given by

$$R_{contact} = R_{Gr/GDL} \cdot A_{GR/GDL} \quad (6)$$

where $A_{GR/GDL}$ is the contact area between the flat graphite plate and the GDL.

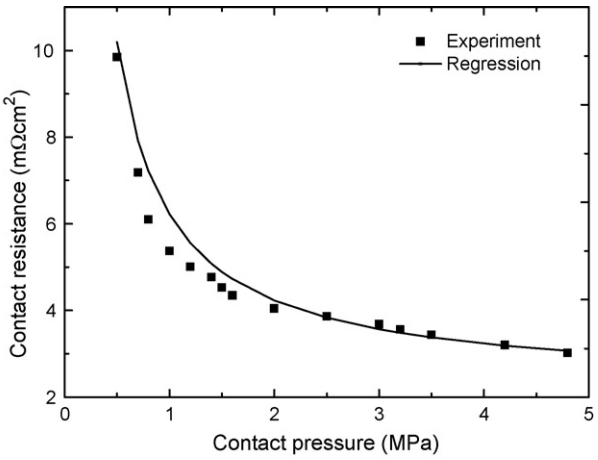

Fig. 3. Constitutive relation of contact resistance vs. contact pressure.

2.1.4. Experiment results

The experimental constitutive contact resistance between the flat graphite plate and the GDL, $R_{contact}$ calculated from Eq. (6), versus contact pressure is shown in Fig. 3. The constitutive relation can be modeled using the least squares (LS) method as

$$R_{contact} = 2.2163 + \frac{3.5306}{p_{contact}} \ (m\Omega\ cm^2) \quad (7)$$

where $p_{contact}$ is the contact pressure. The LS relation of constitutive resistance versus contact pressure (Eq. (7)) is similar in structure to the Cooper–Mikic–Yovanovitch model [5] and the Majumdar–Tien fractal model [6,7].

The experimental constitutive relation can be analyzed in two regions. When the contact pressure changes from 0.5 to 1.0 MPa, the constitutive contact resistance decreases very fast, from 9.847 to 5.376 $m\Omega\,cm^2$. When the contact pressure increases further, the constitutive contact resistance keeps decreasing but much slower. Until the contact pressure reaches nearly 3.0 MPa, the constitutive contact resistance remains almost unchanged. This phenomenon is consistent with the results of Ref. [12]. At this stage if higher contact pressure were applied, the contact area would not increase significantly. No further increase in pressure is carried out since it may result in damage to the GDL.

The experimental constitutive relation of contact resistance between the graphite plate and the GDL versus the contact pressure as shown in Fig. 3 is combined with a simplified prediction and FEM analysis of contact pressure to obtain the contact resistance in the fuel cells.

2.2. Simplified prediction of the contact resistance in a PEM fuel cell assembly

In a practical PEM fuel cell stack, the contact pressure is different from the clamping pressure due to the existence of channels in the BPP. The contact pressure can be obtained according to the clamping pressure and geometry of the bipolar plate. Since the constitutive relation is achieved, the contact resistance can be estimated once the contact pressure is known.

As the contact surfaces of bipolar plate have round corners, the apparent contact area between the graphite BPP and the GDL changes with clamping pressure. The contact area is roughly estimated as the average of these areas with and without round corners and the clamping pressure loaded on the graphite bipolar plate is assumed to be uniformly distributed.

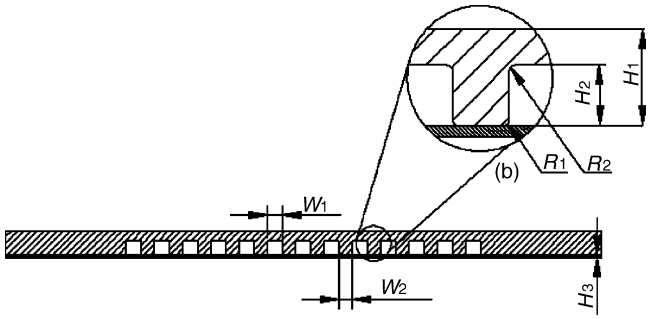

Fig. 4. Schematic of geometry parameters of the graphite BPP/GDL assembly.

The contact pressure can be obtained by

$$p_{clamp} \cdot A_{clamp} = p_{contact} \cdot A_{contact} \quad (8)$$

where p_{clamp} is the clamping pressure, A_{clamp} the area of the surface which undergoes the clamping pressure, $p_{contact}$ the contact pressure and $A_{contact}$ is the contact area.

The contact resistance can then be calculated with the estimation of contact area, contact pressure and the constitutive relation.

$$R_{BPP/GDL} = \frac{R_{contact}}{A_{contact}} \quad (9)$$

2.3. FEM analysis of contact resistance in PEM fuel cell assembly

FEM analysis of contact resistance includes setting up of the FEM model for the graphite BPP and GDL assembly (BPP/GDL), simulating the clamping and contacting and calculating the contact resistance. Firstly, the contact area, contact pressure and their distribution between BPP/GDL are acquired with FEM simulation under assembly clamping pressure. Then the contact resistance is computed according to the contact area, the contact pressure of each BPP/GDL contact element and the constitutive relation. The total contact resistance is calculated by considering all contact elements as parallel resistances.

The FEM analysis is carried out for the cathode side of the BPP/GDL assembly with the commercial FEM software ANSYS. The physical–mechanical properties of the materials in the FEM simulation are the same as those in the experiment shown in Tables 1 and 2. The geometrical parameters of the model are measured from a practical graphite BPP, as shown in Fig. 4 and Table 3, which include thickness of graphite bipolar plate (H_1), groove width (W_1) and depth (H_2), land width (W_2),

Table 3
Geometry parameters of the graphite BPP/GDL assembly

Parameters	H_1	H_2	H_3	W_1	W_2	R_1	R_2
Value (mm)	3.20	2.00	0.377	2.00	1.90	0.20	0.20

corner radius (R_1 and R_2) and thickness of gas diffusion layer (H_3).

The FEM model for the assembly is set up according to the geometrical parameters presented in Table 3. Considering the actual condition of PEM fuel cells in assembly, the following assumptions are made:

(a) The contact status between the BPP and the GDL is a stick contact.
(b) Friction is omitted because the contact interfaces of the BPP and the GDL are smooth and the surface-to-surface contact is continuous. The effect of surface roughness on contact resistance is considered in the constitutive relation of contact pressure versus contact resistance.
(c) Three types of pressure distributions are set considering the possible variation of assembly pressure. They are uniform, linear and block distributions, as shown in Fig. 5. The linear and block distributions of assembly pressure have variation of ±20% of nominal or average pressure.
(d) The assembly clamping only causes elastic deformation in the BPP and the GDL. The mechanical properties of the BPP and the GDL are listed in Tables 1 and 2.

In setting up the FEM model, SOLID95 element and free meshing scheme are utilized to mesh the BPP/GDL assembly with 55,055 elements and 100,023 nodes. SOLID95 is a 3-D 20-node structural solid element, which has compatible displacement shapes and is well suited to model curved boundaries. A free meshing scheme can automatically refine the elements on the round corner of the lands of the BPP to fit contact. The mechanical contact between the BPP and the GDL was handled by CONTA174 and TARGE170 contact elements attached on the BPP and on the GDL, respectively. CONTA174 and TARGE170 are 3-D 8-node surface-to-surface contact elements and applicable to 3-D contact coupled structural analyses.

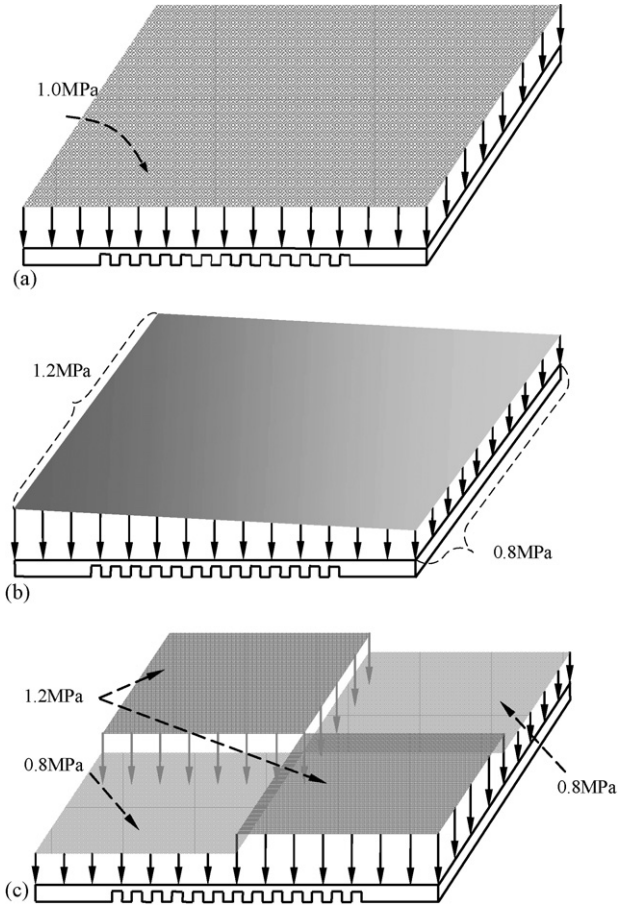

Fig. 5. Distributed form of clamping pressure on the up face of graphite bipolar plate. (a) Uniform distribution; (b) linear distribution; (c) block distribution.

2.4. Experimental verification

In order to validate the results of contact resistance obtained by the simplified prediction and FEM analysis, an experimental verification was conducted by measuring contact resistance between the graphite BPP and the GDL. The material properties, processing conditions and geometry parameters of the graphite BPP and the GDL used in the experiment are consistent with the previous sections. Also the experimental setup and measurement method are the same as in Section 2.1.

The total resistance R_{tot2} of the gold plates/BPPs/GDL assembly is the summation of: (a) the bulk resistance of two graphite BPPs, $2R_{BPP}$, (b) the bulk resistance of the GDL, R_{GDL}, (c) the two interfacial contact resistance between the BPP and the GDL, $2R_{BPP/GDL}$ and (d) the two interfacial contact resistance between gold plate and the BPP, $2R_{Au/BPP}$

$$R_{tot2} = 2R_{BPP} + R_{GDL} + 2R_{BPP/GDL} + 2R_{Au/BPP} \quad (10)$$

The calculation of $R_{BPP/GDL}$ is the same as $R_{Gr/GDL}$. Since the graphite BPP used in experimental validation only has grooves on the contact side with the GDL and is flat on the other side contacted with the gold plate, and it is of the same material and processing conditions as those of the flat graphite plate, $R_{Au/BPP}$ is equal to $R_{Au/Gr}$ in Section 2.1. The resistance $R_{BPP/GDL}$ can be calculated by Eq. (11).

$$R_{BPP/GDL} = \frac{R_{tot2} - R_{BPP} - R_{GDL} - R_1}{2} \quad (11)$$

3. Results and discussion

3.1. FEM simulation results of contact pressure

During assembly, it is possible for the clamping pressure to have some variation. In this study three types of clamping pressure distribution are considered, which are a uniform distribution, a linear distribution and a block distribution, as shown in Fig. 5. All three distributions have the same average value of clamping pressure.

From the FEM simulation results, not only can the contact resistance be calculated but the contact pressure can also be obtained. The contact pressure between the graphite BPP and the GDL under the three different types of clamping pressure is shown in Fig. 6. It can be seen that the contact pressure distribution has the same distribution of the loading form. The largest contact pressure lies in grooves of the graphite BPP.

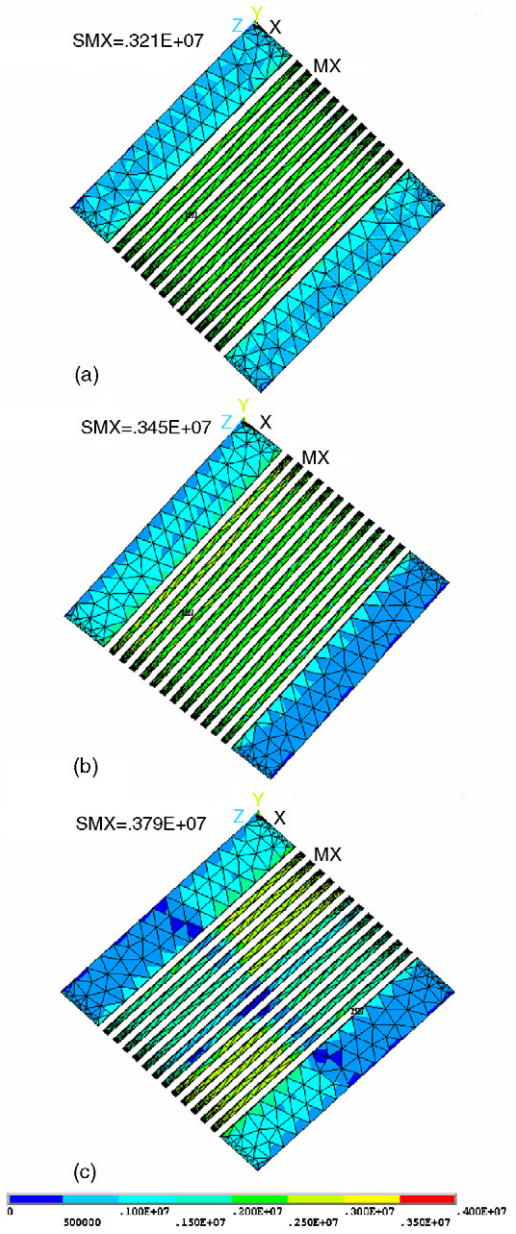

Fig. 6. Distribution of contact pressure of FEM simulation under different loading condition. (a) Uniform distributed loading; (b) linear distributed loading; (c) block distributed loading.

3.2. Comparison between the contact resistances by FEM analysis, simplified prediction and experiments

The contact resistance between the BPP and the GDL from the FEM analysis under different loading forms, the simplified prediction of the contact resistance and the results of the experimental verification are shown in Fig. 7. The results of the FEM analysis and the simplified prediction are shown to be reasonably accurate compared with the experimental results. This indicates that these two semi-empirical estimation methods take into account the major influencing factors involved in the contact phenomena. Furthermore, there is very little difference among the three curves marked with triangles which represent the FEM analysis results under different assembly clamping pressure distributions. The contact resistance is greatly influenced by the average value of assembly clamping pressure but rarely by its variation. That is, the contact resistance is robust to the assembly clamping pressure distributions.

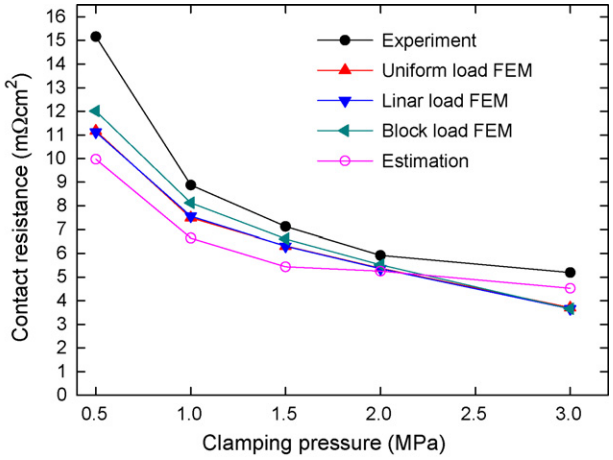

Fig. 7. Contact resistances by experiment, FEM analysis and simplified prediction.

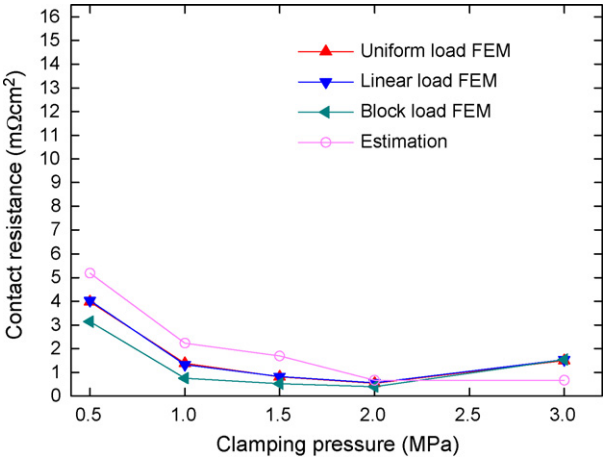

Fig. 8. Deviations of contact resistances by the FEM analysis and the simplified prediction from experiments.

In order to further compare the three types of results, the deviations of the results by the FEM analysis and the simplified prediction from experiments are compared in Fig. 8. It can be seen that the simplified prediction method is robust though it has a little more deviation than the FEM simulation.

This methodology may be applied to predict the contact resistance between any other GDLs and BPPs of different materials and with various channel geometries and configurations. As long as the experimental constitutive relation is obtained, both the FEM analysis and the simplified prediction may effectively estimate the contact resistance. In particular, the simplified prediction method provides an efficient approach to estimate the contact resistance.

4. Conclusions

Two semi-empirical methods for estimating the contact resistance between a BPP and a GDL are proposed using an

experimentally acquired contact resistance–pressure constitutive relation. The proposed methods circumvent the difficulties of dealing with complex material and geometrical variations for contacting bodies and are shown to be effective in predicting the contact resistance of PEM fuel cells since good agreement was demonstrated between the predications and the experimental results.

The simplified prediction method provides an efficient approach to estimate the contact resistance using only the area of the BPP, the estimated area of contact between BPP and GDL, the assembly clamping pressure and the experimental contact resistance–pressure constitutive relation.

The contact resistance is greatly influenced by the average value of the assembly clamping pressure. Variation of the assembly clamping pressure has a small impact on the contact resistance. The contact resistance is robust to assembly clamping pressure distributions.

The methodology of the present study, in addition to predicting the contact resistance, can be used to model the assembly process and to optimize the assembly pressure to improve the performance of PEM fuel cells.

Acknowledgements

The work reported here is sponsored by the Specialized Research Fund for the Doctoral Program of Higher Education of the Ministry of Education of China, Grant No. 20050056006, and the Cheung Kong Scholars Programs of China's Ministry of Education and Tianjin University. The authors gratefully acknowledge these supports.

References

[1] G. Hoogers, Fuel Cell Technology Handbook, CRC Press, Boca Raton, FL, 2003.
[2] http://bama.ua.edu/∼rreddy/projects/fuel_cells.htm.
[3] J.A. Greenwood, J.B.P. Williamson, Contact of nominally flat surfaces, Proc. R. Soc. Ser. A 295 (1966) 300–319.
[4] J.A. Greenwood, J.B.P. Williamson, Br. J. Appl. Phys. 17 (1966) 1621–1632.
[5] M.G. Cooper, B.B. Mikic, M.M. Yovanovich, Int. J. Heat Mass Transfer 12 (1969) 279–300.
[6] A. Majumdar, C.L. Tien, Wear 136 (1990) 313–327.
[7] A. Majumdar, C.L. Tien, J. Heat Transfer 113 (1991) 516–525.
[8] W.K. Lee, C.H. Ho, J.W. Van Zee, M. Murthy, J. Power Sources 84 (1999) 45–51.
[9] J. Ihonen, F. Jaouen, G. Lindbergh, G. Sundholm, Electrochim. Acta 46 (19) (2001) 2899–2911.
[10] H.L. Wang, M.A. Sweikart, J.A. Turner, J. Power Sources 115 (2003) 243–251.
[11] E.A. Cho, U.-S. Jeon, H.Y. Ha, S.-A. Hong, I.-H. Oh, J. Power Sources 125 (2004) 178–182.
[12] V. Mishra, F. Yang, R. Pitchumani, ASME J. Fuel Cell Sci. Technol. 1 (2004) 2–9.
[13] S.J. Lee, C.D. Hsu, C.H. Huang, J. Power Sources 145 (2005) 353–361.
[14] G.B. Jung, A. Su, C.H. Tu, F.B. Weng, S.H. Chan, Innovative flow field combination design on direct methanol fuel cell performance, in: Proceedings of the Third International Conference on Fuel Cell Science, Engineering and Technology, Ypsilanti Marriott Hotel at Eagle Crest-Ypsilanti, MI, May 23–25, 2005, pp. 1–6.